


RESEARCH ARTICLE

Fiber optic health monitoring and temperature behavior of bridge in cold region

Feng Xiao¹  | J. Leroy Hulsey¹ | Radhakrishnan Balasubramanian²

¹Department of Civil Engineering,
University of Alaska Fairbanks, Fairbanks,
Alaska 99775, USA

²State of Alaska DOT&PF, 3132 Channel
Drive, Juneau, Alaska 99801, USA

Correspondence

Feng Xiao, Department of Civil Engineering,
University of Alaska Fairbanks, Fairbanks,
Alaska 99775, USA.
Email: xfeng2@alaska.edu

Funding Information

Alaska University Transportation Center,
Grant/Award Number: 510015

Summary

The objectives of this research are (a) to establish a structural health monitoring system for bridge safety evaluation that is suitable for cold, remote regions and (b) to identify the bridge responses under variations in temperature. To achieve this, fiber optic sensors with temperature compensation were selected that were suitable for cold regions. This technique allows monitoring equipment to operate far from the sensor installation site, which avoids exposing much of the equipment to extremely cold temperatures and makes a power supply more accessible. The bridge temperature behavior is studied based on the real-time field measurement data, and the relationship between the thermal loading and the bridge response is presented.

KEYWORDS

bridge response, cold regions, fiber optic, structural health monitoring, temperature measurement

1 | INTRODUCTION

Bridge health monitoring systems can provide an early warning for bridge safety issues and are used to monitor structural conditions and changes in real time.^[1,2] They can also provide engineers with valuable data for asset management plans and bridge service life studies. Structural health monitoring (SHM) systems have been widely applied for use in bridge condition evaluation.^[3–8] However, the application of these systems in cold regions is lacking, and very few quantitative studies have examined the temperature behavior of large-scale bridges.^[9] The modern transportation system has been extended to both cold and hot extremes; thus, bridge research in those areas should attract attention. The core theme of this paper is to establish a SHM system for bridge safety evaluation that is suitable for cold, remote regions and to identify the bridge response from the variations in temperature.

Bridges in Alaska are subjected to extremely low temperatures. During the first decade of the 21st century, most of Alaska experienced a cooling shift that modified the long-term warming trend.^[10] Bridges may be located in permafrost areas, where there can be excessively deep snow, strong winds, and even seismic events. Bridges in these harsh

conditions are often located in remote areas, and difficulties arise when monitoring such bridges because the harsh environment affects the reliability and durability of SHM equipment, sensors, and data communication tools. This study applied a fiber optic real-time monitoring system for a highway bridge located in Alaskan permafrost. Based on a 2-year, real-time monitoring project (from fall 2012 to spring 2014), this system proved that it can provide stable and reliable data for bridge evolution and is suitable for cold and remote conditions. The first part of this research provided guidelines for the implementation of bridge health monitoring in cold, remote regions.

In addition to the effect of cold temperature and remote locations, Alaska experiences a polar day and night. This phenomenon contributes to the unusual solar radiation conditions in this area. The bridges are subjected to continuous temperature variations primarily due to solar radiation and ambient air temperature. Because of Alaska's high latitude, there is a large variation in daylight between summer and winter, which produces unusual solar radiation conditions. The effects of cold temperature, remoteness, and the polar day and night in Alaska may induce changes in conditions that are not typically found elsewhere.

Studies of thermal loads for different bridges subjected to changing environmental factors have been performed worldwide. Past research can be roughly divided into three categories: theoretical methods,^[11,12] numerical approaches, and field measurements. The theoretical method, which employs a series of assumptions, pursues closed-form solutions of the heat transfer equation and reveals the temperature distribution in bridges. The numerical approach, which can give acceptable results if input parameters are adjusted properly, solves the heat transfer equation by using the finite element or finite difference method. Finally, field measurements, which provide the most meaningful thermal load of bridges, obtain the temperature distribution by using temperature sensors that are installed on full-scale bridges in real environments. Each method has its advantages and disadvantages.^[13] In this research, field-measured temperatures were obtained for a steel–concrete composite bridge using 11 fiber optic temperature sensors. Sensors had already been distributed on the bridge in longitudinal and transversal directions. Real-time temperature data, combined with other static and dynamic measurement data, were recorded on a remote computer, and the relationship between thermal loading and bridge response was established.

2 | FIBER OPTIC WITH TEMPERATURE COMPENSATION

Foil strain gauges are the most common type of strain gauge and consist of a thin insulating backing that supports a fine metallic foil. However, their long-term performance is not good, particularly in harsh environments.^[14] The available systems in applications to bridges in cold and remote regions of Alaska have been studied, and the fiber optic sensor workability in the cold regions has also been demonstrated.^[15] Fiber optic sensors can be used to measure strain, temperature, accelerometer, displacement, and other quantities. They also have durability in harsh environments, where the operating temperature range can be between -40 and 176 °F. This technique has been applied for SHM in low-temperature conditions.^[16–18]

2.1 | Fiber optic advantages

Fiber optics sensors are stable compared with the traditional foil strain gauge. The light signal transmits over a very long length with very low signal transmission loss. The fiber optic sensor is composed of glass, and the protection cover is free from corrosion, thus providing long-term stability. Fiber optical sensors have the advantage of being nonconductive, which ensures that they are free from electromagnetic and radio-frequency interference. The fiber optical sensors are practical for use in city areas, which have serious signal

interferences. Fiber optic sensors and cables are also very small and light, thus making it possible to permanently incorporate them into structures. Alternatively, several sensors can be joined into one array, which means that one cable can work for approximately 10 sensors. Compared with the traditional foil strain gauge, which needs two cables for one sensor, the fiber optical system simplifies the cable layout, ultimately shortening the installation period and reducing the installation costs. Figure 1 shows a fiber optic strain sensor on the Chulitna River Bridge.

2.2 | Fiber Bragg grating

There is a fiber Bragg grating in each optical sensor. The fiber Bragg grating is composed of a distributed Bragg reflector, which has a higher refractive index than the rest of the glass core. It only reflects certain type of wavelengths light and transmits all others. The optical sensing interrogator sends the wide-spectrum light to the fiber Bragg grating. Because the distance between each Bragg reflector is constant, only one kind wavelength of light is reflected back to the interrogator. The interrogator receives the wavelength and transfers it to a digital signal. There are several external factors, which can change the distance between each Bragg reflector including such as strain and temperature. The reflected wavelength of light will increase if the distance is increased. In the same way, the reflected wavelength of light will decrease if the distance of the Bragg grating decreases. An optical sensing interrogator indicates the changing of wavelength and transfers it to the digital signal. The fiber Bragg grating transfers the changing of strain or temperature to the changing of light wavelength. The optical sensing interrogator then transfers the changing of light wavelength to digital data, and a local computer analyzes and records the sensing information.

2.3 | Fiber optic sensor array

The optical sensing interrogator sends a wide-spectrum light with a wavelength range from 1510 to 1590 nm. The optical sensor reflects only certain wavelengths of light back to the interrogator, and other wavelengths of light pass through the sensor. The changing of strain or temperature changes only the reflected light wavelengths by approximately 5 nm such that one optical sensor only uses 5 nm of wavelength range. However, there is a range of 75-nm wavelengths that can still be used for measurement. More fiber optical sensors can be placed after this sensor and reflect other ranges of light wavelengths to the interrogator. Normally, there is a 5-nm wavelength spacing between each sensor. In this condition, approximately eight fiber optical sensors can be put into use in one fiber optical cable and work as one fiber optical sensor array.

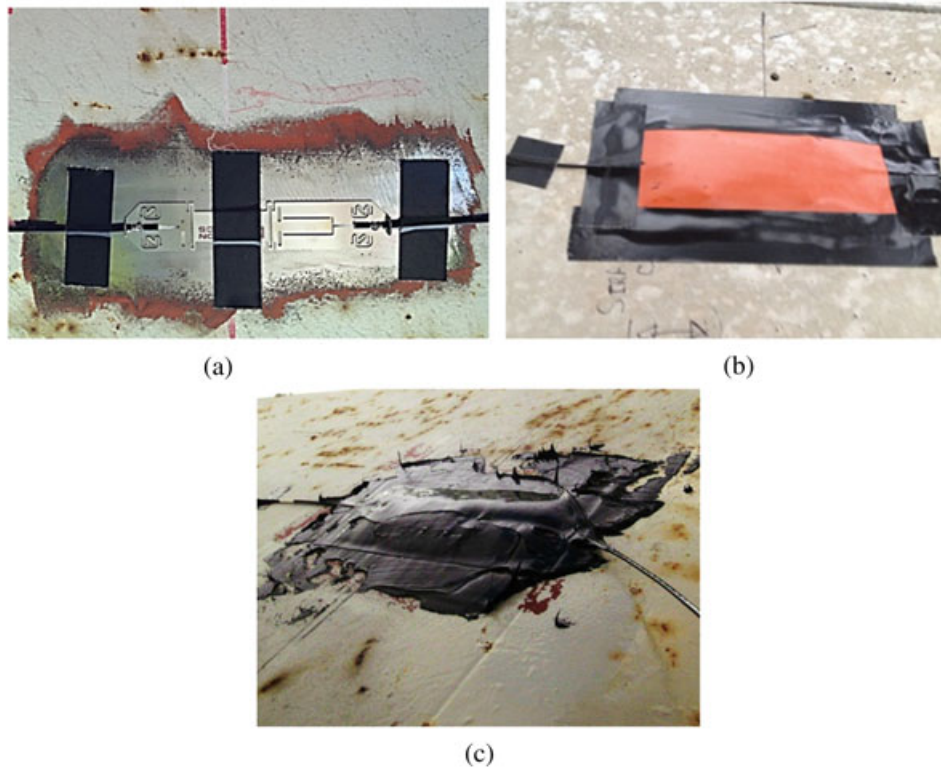


FIGURE 1 Fiber optic strain sensor and covered with the protection

2.4 | Temperature compensation

Fiber optics sensors respond to both temperature- and mechanically induced strains. The temperature-induced strain is a combination of two factors. First, the relative difference in the coefficients of thermal expansion between the gauge and the measurement substrate on which it is mounted causes a strain to be induced in the gauge as temperature changes. Second, the index of refraction of the Bragg grating is a function of temperature that causes the center wavelength to shift. There are several methods used to determine the thermal output of a gauge. Once the thermal output is known, the mechanically induced strain can easily be calculated by subtracting the thermal output from the measured strain. The relationship between wavelength and strain for a fiber optic gauge is

$$\varepsilon = (10^6 \mu\text{m/m}) \frac{\Delta\lambda/\lambda_0}{F_G} - \varepsilon_{T0}, \quad (1)$$

where $\Delta\lambda$ is the wavelength shift (nm), λ_0 is the initial reference wavelength (nm), F_G is the gauge factor, and ε_{T0} is the thermal output ($\mu\text{m/m}$). The thermal output can be estimated if the coefficient of thermal expansion of the substrate and the gauge constants are known. A temperature compensation sensor was integrated inside the strain gauge (Figure 1a). Measurements of relative temperature were used to compensate for strain measurements. Additional

temperature sensors were in close proximity to the strain sensors to improve the accuracy of the strain measurement.

3 | SEPARATED MONITORING EQUIPMENT

This section introduces a new method to separate the monitoring equipment from the bridge site. The purpose is to solve the SHM application problems in cold and remote areas. Limited access to power and harsh weather conditions can damage the equipment. Traditionally, the monitoring system could not be separated from the bridge site because the field-measured electrical signal would drift over a long-distance translation. That required a computer transfer from electrical signal to digital signal before the signal drift and thus required the local computer to be installed on the bridge site to conduct this translation. The local computer would then send the digital data to a remote computer with the traditional wired sensor network or the wireless sensor network.^[19,20]

However, cold and remote bridge site conditions make it difficult to place monitoring equipment on such bridges. First, there is limited power on site to support the local computer and interrogator, and the nearest power station is several miles away. The electrical or wireless signal would drift before connecting to the monitoring equipment. Second, the extremely low temperature on the bridge site would make

it difficult for the computer and interrogator to work properly. The cold temperature can damage the local computer and interrogator.

Considering these factors, fiber optics were selected for bridge monitoring in cold remote areas. Fiber optics use light signals for transmission, and the signal can transfer over long distances before it becomes unstable. The fiber optics are composed of three layers: the core, the cladding, and the buffer coating. The core is high-density glass, in which light travels. The cladding is low-density glass and reflects the light into the core. The buffer coating is a plastic coating that is used to protect the fiber from external damage. Because the glass core has a higher refractive index than the glass cladding does, light is reflected in the glass core, and the glass cladding does not permit the escape of any light from the glass core. In this way, light can travel great distances in the glass core.

The fiber optic signal behavior is stable over long-distance transformations. It has already been demonstrated that optical carriers can transfer radio-frequency and microwave signals up to hundreds of kilometers and over dedicated fiber routes.^[21] Lopez *et al.*^[22] proved the ultra-stable transfer of an optical frequency over 540 km. A significant gain can be achieved using the very high frequency (~200 THz) of the optical carrier to transfer an ultra-accurate and stable frequency reference over long distances.^[22] The long-distance stability can make it possible to separate the monitoring system from the sensor installation location by a large distance.

Fiber optic sensing solutions provide benefits over electrical solutions in terms of allowing the instrumentation electronics to be located far from the sensor installation. In this case, the instrumentation was over 1.5 miles away at the Denali Princess Wilderness Lodge because the site contained power and internet access. The instrumentation was integrated with the sensors via fiber optic cables that were already installed along the roadway leading to the bridge. The local computer in the Princess Hotel transferred the fiber optic signal to the internet and uploaded it (Figure 2).

The fiber optic SHM system is composed of five parts: the optical sensing interrogator, channel multiplexer, optical sensors, local computer, and remote computer (Figure 2). The optical sensing interrogator sends a wide wavelength swept laser and synchronizes measuring the reflected laser, and it then transfers the light signal to a digital signal. The channel multiplexer expands fiber connections.

The optical sensing interrogator in the Princess Hotel (Figure 3) sends four optical signals (laser) to the channel multiplexer at the bridge site (Figure 4). The multiplexer has four switchers that switch each laser among four channels such that the total channel number is increased to 16. The laser comes to each sensor after the multiplexer. There is an optic Bragg grating in each optical sensor that can reflect certain wavelengths of light back to the interrogator; other wavelengths of light will pass through the optic Bragg grating. The interrogator can

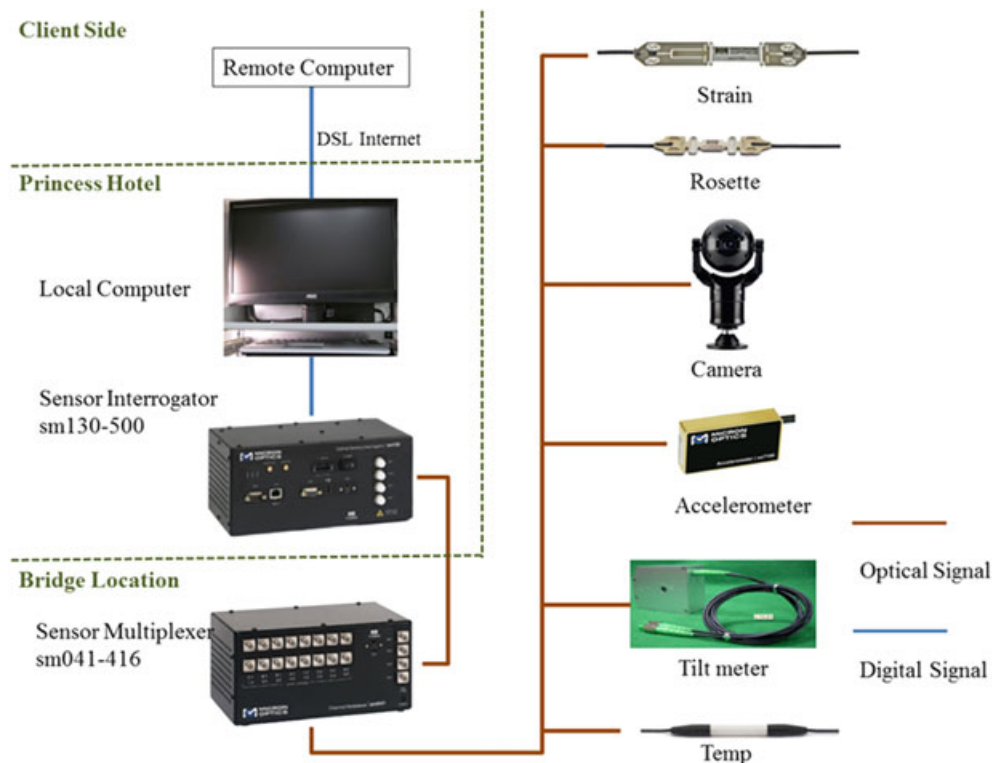


FIGURE 2 System configuration

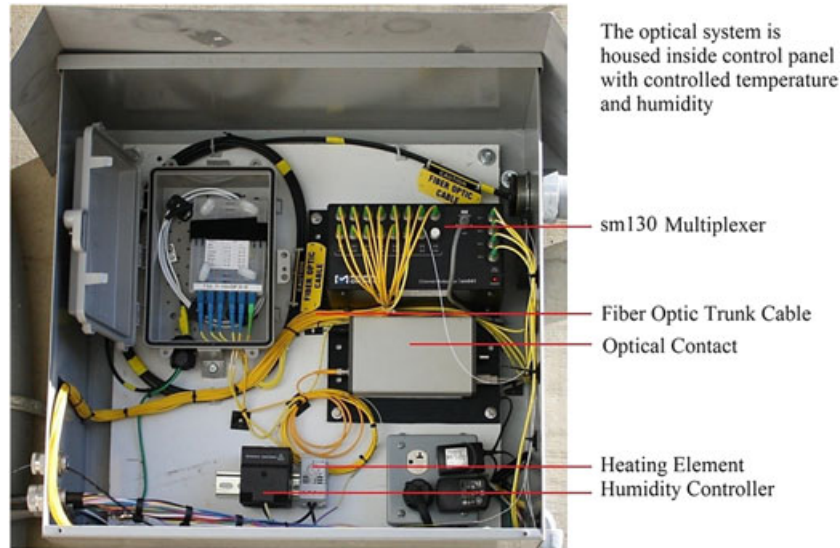


FIGURE 3 Control panel at the bridge

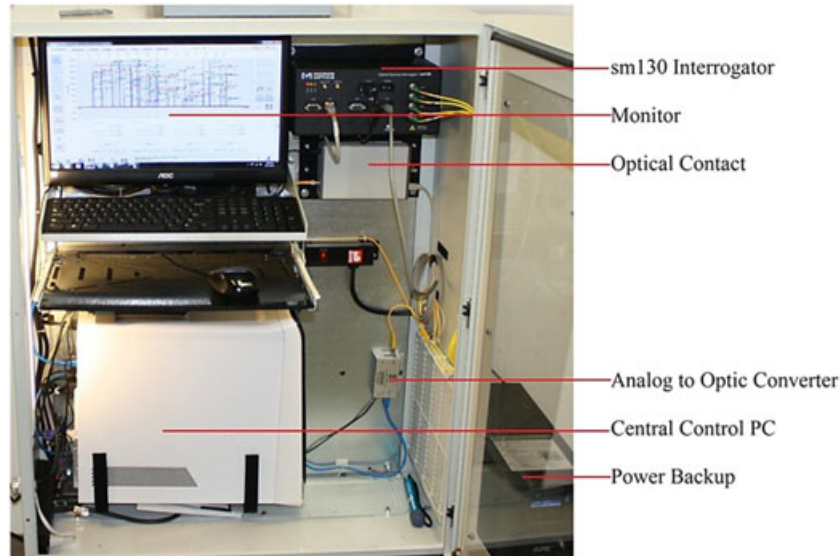


FIGURE 4 Control panel at the Princess Hotel

indicate the change in the optical signal and transfer the optical signal to a digital signal before sending it to the local computer. The local computer analyzes the data and sends the results to the remote computer via digital subscriber line internet.

4 | BRIDGE MONITORING

The 800-ft Chulitna River Bridge, a steel girder plate bridge (Figure 5) located in Trapper Creek, Alaska, is part of the Parks Highway, which links Anchorage to Fairbanks. Heavily loaded vehicles of up to 410,000 lb regularly travel the route. In addition, the region endures large temperature swings, frequent flooding, and annual snow amounts

measured in meters. The closest National Weather Service weather station is located at Talkeetna Airport. National Oceanic and Atmospheric Administration Annual Climatological Summaries from 2005 to 2015 indicate a high temperature of 96 °F and a low of −34 °F. The bridge is located in a permafrost region of Alaska. The local weather requires the SHM system to be durable in low temperatures.

The sensor layout addresses specific issues, that is, overstress of plate girders, load transfer through the cross frame, load distribution in girders and trusses, and truss bearing not being in contact with supports.

There are total of 73 sensors installed for monitoring of this bridge. A previous study was aimed at providing the Alaska Department of Transportation & Public Facilities



FIGURE 5 Chulitna River Bridge

with information to monitor the load shed to the girders caused by the truss's low stiffness relative to girders and truss bearings that are not in contact with supports.^[23] The sensor arrangement (Figure 6) provided information about changes

in the load distribution in girders and trusses. Most of the sensors are located in the places that have low load rating factors, and the others are used to indicate the load distribution of the bridge.

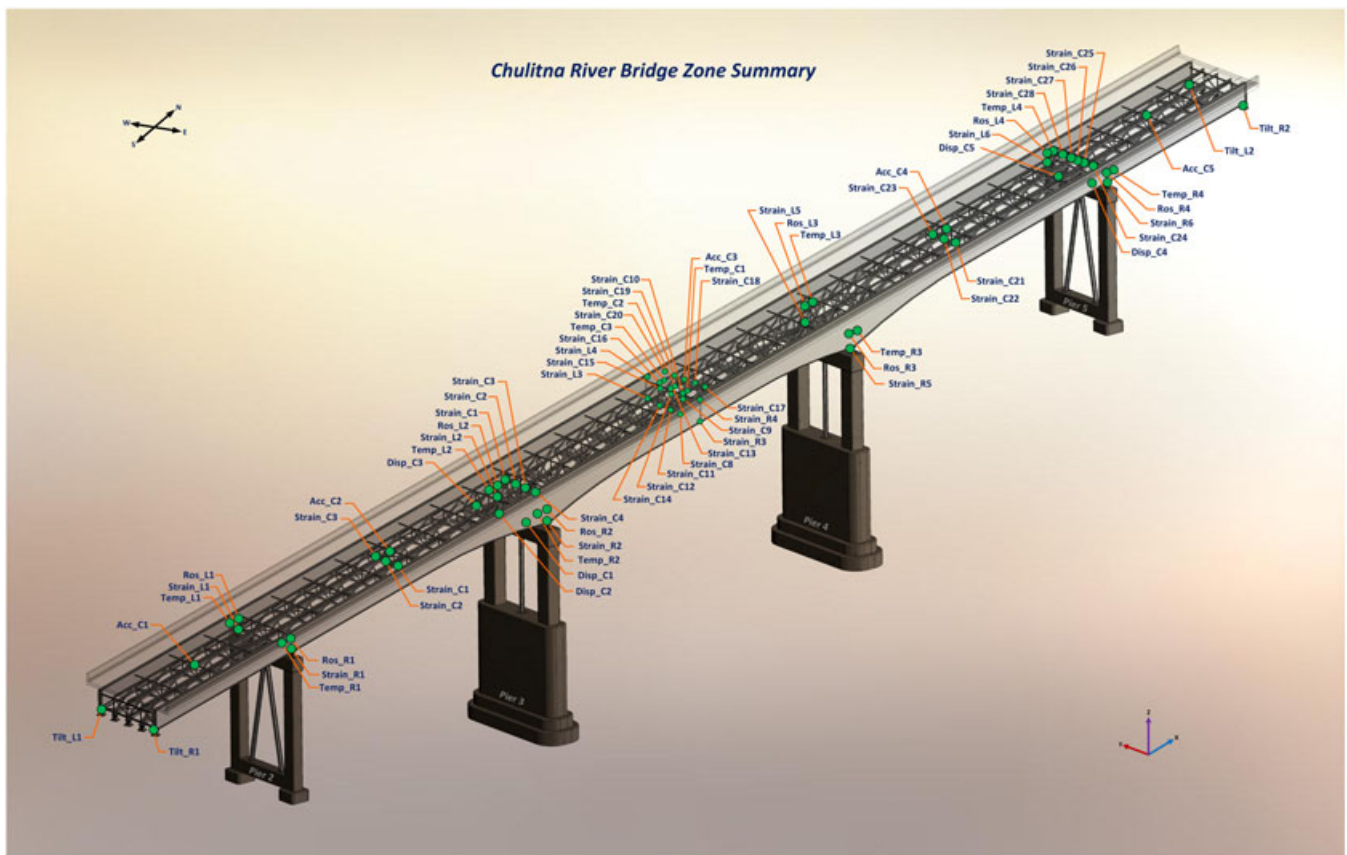


FIGURE 6 Fiber optic sensor layout

Eight optical rosette strain sensors combined with 12 optical strain sensors are placed near the piers and middle of the girders to monitor the bending and shear force. Fifteen optical strain sensors are located in the composite trusses that can monitor the bending and axial force. The live load distribution in the girders and the trusses can be calculated by comparing the force between the girders and the trusses. To monitor the load transfer through the cross frames and the concrete deck, 12 optical sensors are placed on the cross frames' diagonal trusses and the concrete deck. Other optical sensors are located in the member, which shows a low load rate. Five accelerometers are installed to monitor the changing stiffness in the trusses and girders. The supports are monitored for rotation with tiltmeters. If all supports are not free to rotate as they should, the bridge may exhibit a twisting condition. This accounts for an additional four sensors. Five displacement monitors monitor the vertical movement of the truss bearing.^[24]

5 | TIME-DEPENDENT TEMPERATURE BEHAVIOR

Temperature variation affects bridges in a complicated manner. From the point of view of global response, uniform temperature changes cause a large overall expansion and contraction in bridge components and bending in the vertical plane.^[13] First, such bending has a significant influence on the structural dynamic characteristics.^[25–29] Second,



FIGURE 7 Steel-concrete composite condition

TABLE 1 Record of climatological observation

Day		4/19/2013	4/20/2013	4/21/2013	4/22/2013
Air temperature °F (°C)	Max	48 (9)	45 (7)	46 (8)	47 (8)
	Min	23 (–5)	17 (–8)	14 (–10)	19 (–7)
Precipitation (in.)		0.00	0.00	0.00	0.00

continuing thermal expansion and contraction are often accompanied by large forces that may damage critical bridge members such as expansion joints, bearing supports, and wearing surfaces.^[30]

The steel-concrete composite bridge is composed of steel beams and concrete slabs. Figure 7 shows the steel-concrete composite condition of the Chulitna River Bridge. The different heat transfer coefficients of steel and concrete make a nonlinear thermal gradient along the vertical axis of the cross section. As a result, the model of thermal load is different from that in a homogeneous material. In a composite bridge, the thermal stresses were found to be comparable to the dead load and live load stresses. Therefore, the thermal load in steel-concrete composite bridges is particularly important.^[13] Emanuel and Hulsey^[11] used equations to simulate these weather extremes, and finite element analysis was used to calculate bridge temperatures as a function of time. Hulsey^[12] established an empirical time-dependent equation for ambient air temperature, solar radiation, wind speed, and time-dependent models for highway structures.

5.1 | Ambient air temperature

The air temperature is analyzed by using the closest Talkeetna weather station, which is operated by a professional meteorologist from the National Weather Service (National Oceanic and Atmospheric Administration Government Agency). There are 20 such stations fairly well distributed over the different climatic zones of Alaska.^[31] Table 1 shows the record of climatological observation from April 19, 2013, to April 22, 2013.

5.2 | Measured temperature

There are 11 temperature sensors (Figure 8) distributed along the bridge's longitudinal and transversal directions to monitor the time-dependent temperature distribution. The location of sensors is shown in Figure 6. Figure 9 shows real-time monitoring data from the temperature sensors.

The sensors show the generally observed “sinusoidal-type” fluctuations of temperature. However, some sensors, such as R1, R2, and R4 at the east side girder and L3 and L4 at the west side girder, show bumps in the measurement because of the sunlight effect. The temperature sensor readings show the local temperatures are highly variant due to the direction of sunshine. The first bump of sensor R1,



FIGURE 8 Temperature sensor

R2, and R4 are caused from the sunrise. The second bump of sensor L3 and L4 are in response to the sunset from the west direction. The daily transverse temperature difference

between outside girders is 23 °C. Sensors C1, C2, and C3 are located on the stringers (Figure 7) at the bottom of bridge, and the temperature is lower than the outside girder's temperature. The largest temperature difference between the bridge bottoms to the outside girder can reach 23 °C.

On the other side, the temperature in the longitudinal direction is different: temperature R1, R2, and R3 are distributed at the east side of bridge outside girder, where the temperature changes consistently based on weather conditions, but the amplitude of variations is different. The largest longitudinal temperature variation of 17 °C is found

TABLE 2 Bridge thermal expansion by using tiltmeters

	Tilt R1	Tilt L1	Tilt R2	Tilt L2
Maximum reading (°)	1.731	1.896	1.889	1.997
Minimum reading (°)	-0.085	-0.071	-1.348	-1.624
Longitudinal movement (in.)	0.38	0.42	0.68	0.76

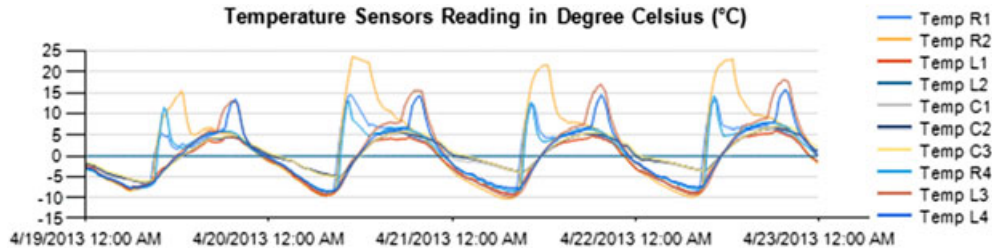


FIGURE 9 Temperature sensor readings

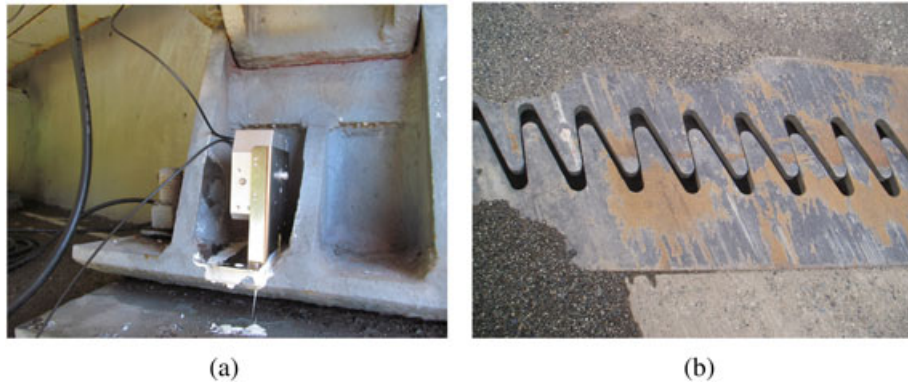


FIGURE 10 Photographs (a) spacing between deck and abutment and (b) tiltmeter on the roller support

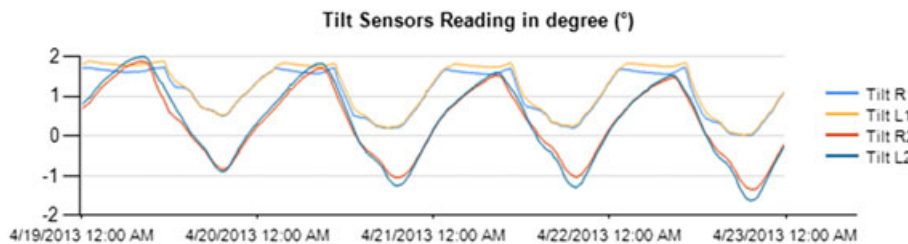


FIGURE 11 Tilt sensor readings

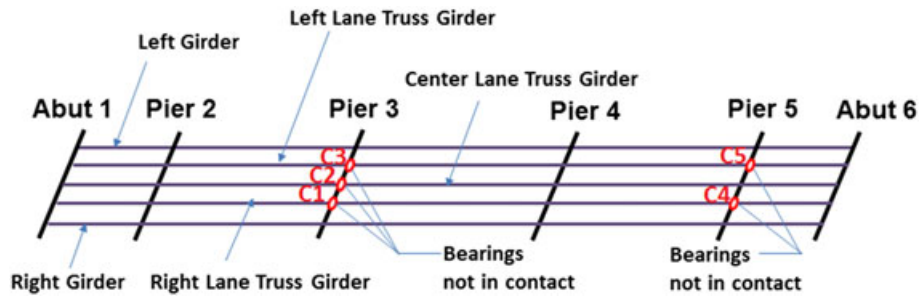


FIGURE 12 Locations of bearing not in contact

in the outside girder. Based on the time-dependent measured temperatures, the bridge temperature distribution differs in the transversal and the longitudinal direction.

Table 1 shows that the 4-day highest air temperature is 48 °F (9 °C) and that the lowest temperature is 14 °F (−10 °C), and Figure 9 shows that the extreme bridge measured temperatures are 73 °F (23 °C) and 12 °F (−11 °C). Compared to this period of data, the measured temperature can be 34% higher than the air temperature and 9% smaller in the lower bound. There exists a significant difference between the air temperature and the bridge temperature, mainly because of solar radiation. The bridge as is temperature must be verified instead of using air temperature in the thermal loading design.

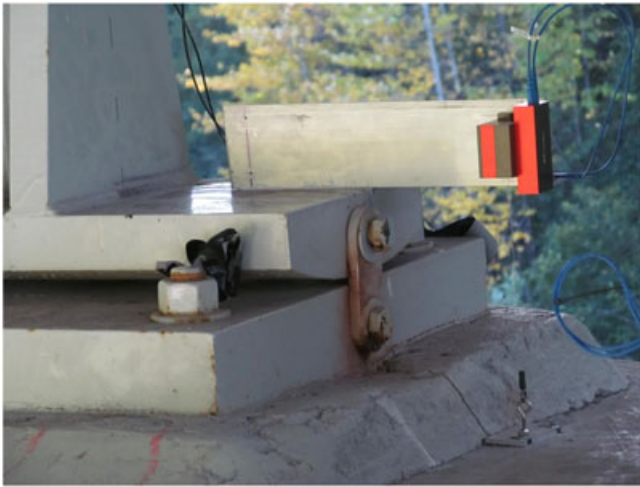


FIGURE 13 Displacement sensor on a roller support

5.3 | Thermal expansion and contraction

Four tiltmeters were installed on the bridge roller supports (Figure 10a), which rotate in response to the thermal expansion during daily temperature changes (Figure 11). There is a spacing (Figure 10b) between the bridge deck and the abutment to accommodate this longitudinal movement.

Figure 11 shows that the movement of the bridge support is largely determined by the thermal expansion of the entire bridge and that the traffic loading has limited influence in comparison. The expansion of the bridge is the result of composite local thermal expansion. The rotation recorded by each roller support at the abutment is shown in Table 2. The radius of the roller is 12 in., and the equivalent longitudinal displacements at each tiltmeter is calculated.

5.4 | Thermal bending and torsion

Temperature variations cause the bridge to bend in the vertical plane. There are five roller supports at piers 3 and 5 that are either not or partially in contact with bridge piers (Figure 12). Displacement sensors were installed at those locations to monitor the vertical movements (Figure 13). Figure 14 shows the real-time vertical movements from the displacement sensors.

Bearing support vertical movements are highly dependent upon both the thermal loading and the influence of traffic loading. On this bridge, the variation of vertical movements appears to be highly dependent on the temperature change. The largest measured movement was 12 mm at displacement

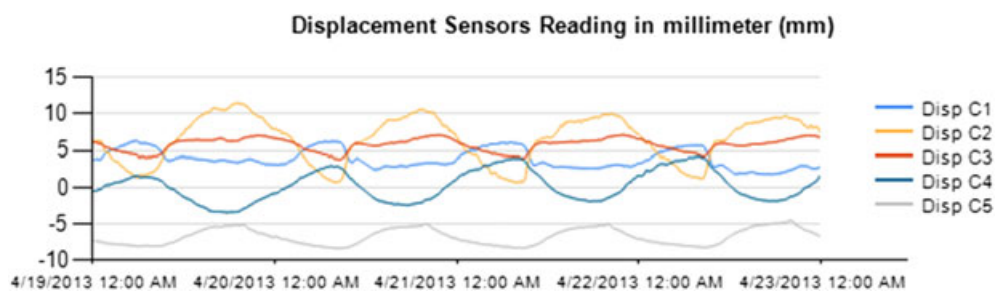


FIGURE 14 Displacement sensor readings

sensor C2. Figure 12 shows the displacement sensors C4 and C5 along the same cross section of pier 5, but the displacement sensor movements developed in a contradictory direction (Figure 14). The data suggest that there is torsion at the cross section of pier 5, which is caused by thermal loading. This phenomenon also happens at the pier 3 cross section, based on the vertical movement measured by sensors C1, C2, and C3 (Figure 14).

6 | CONCLUSION

An Alaskan bridge located in a cold and remote area with limited access to power and the harsh weather conditions can damage structural health monitoring equipment. Fiber optic technology has the capabilities of long-distance transmission, which can separate the SHM system to a distance of 1.5 miles away from the bridge site. The structural health equipment was stored in the Princess Hotel in this case to keep it in a safe condition.

The distribution of temperature on the bridge is not only dependent on the daily temperature but also determined by the sunlight direction. The local temperature is highly variable as a result of sunlight direction and sensor location. The transverse temperature difference was 23 °C. The temperature difference between the outside girder and bridge bottom was as high as 23 °C. The longitudinal temperature variation was 17 °C. The local temperature was required to adjust fiber optic sensor's accuracy near the spot of measurement.

The measured bridge temperatures had a significant difference compared to the air temperature. Based on 4 days of real-time temperature data in April 2013, the maximum measured bridge temperature reached levels up to 34% higher and 9% lower than the air temperature. This is large due to solar radiation, and the relationship between the air temperature and bridge thermal distribution must be studied in different regions.

In addition, this region endures large temperature swings, which causes thermal expansion to determine the bridge's longitudinal movement, bending, and can create torsion. There was limited movement caused by traffic loading compared with thermal loading. The bridge longitudinal movement was 0.76 in. (19 mm), and the vertical movement was 0.47 in. (12 mm) based on a variation of air temperature from 48 to 14 °F. This shows the potential for a large movement under an annual temperature variation from 96 to −34 °F. The capability of bridge movement should be studied in the future based on historical temperature variations.

This paper presents a bridge health monitoring system for cold, remote areas and considers the thermal loading relationship with the bridge behavior. The bridge thermal

loading model and the comparison of measurements require further investigation because they were not concluded in this study.

ACKNOWLEDGMENTS

Support of this research by the Alaska University Transportation Center grant no. 510015 is gratefully acknowledged. The writers wish to acknowledge support from the Alaska Department of Transportation & Public Facilities, University of Alaska Fairbanks, University of Alaska Anchorage, Alaska Native Science and Engineering Program, Chandler Monitoring System Inc., and Micron Optic, Inc.

REFERENCES

- [1] F. Moreu, R. E. Kim, B. F. Spencer, *Struct. Control Health Monit.* **2017**, 24(2).
- [2] F. Ansari, *Smart Mater. Struct.* **2005**, 14(3), S1.
- [3] M. Modares, N. Waksanski, *Pract. Period. Struct. Des. Constr.* **2012**, 18(3), 187.
- [4] H. N. Li, L. Ren, Z. G. Jia, T. H. Yi, D. S. Li, *J. Civil Struct. Health Monit.* **2016**, 6(1), 3.
- [5] F. Xiao, J. L. Hulsey, G. S. Chen, *Appl. Phys. Res.* **2015**, 7(1), 47.
- [6] F. Xiao, G. S. Chen, J. L. Hulsey, J. D. Dolan, Y. Dong, *Adv. Struct. Eng.* **2016**, 19(4), 660.
- [7] J. T. Huffman, F. Xiao, G. Chen, J. L. Hulsey, *J. Civil Struct. Health Monit.* **2015**, 5(4), 389.
- [8] S. Nagarajaiah, K. Erazo, *Struct. Monit. Maint.* **2016**, 3(1), 51.
- [9] Y. Xia, B. Chen, X. Q. Zhou, Y. L. Xu, *Struct. Control Health Monit.* **2013**, 20(4), 560.
- [10] G. Wendler, L. Chen, B. Moore, *Open Atmos. Sci. J.* **2012**, 6, 111.
- [11] J. H. Emanuel, J. L. Hulsey, *J. Struct. Div.* **1978**, 104, 65. ASCE 13474 Proceeding.
- [12] J. L. Hulsey, D. T. Powell, *Transp. Res. Rec.* **1993**, (1393).
- [13] G. D. Zhou, T. H. Yi, *Int. J. Distrib. Sensor Netw.* **2013**, 22, 2013.
- [14] Y. L. Xu, Y. Xia, *Structural Health Monitoring of Long-span Suspension Bridges*, CRC Press **2011**.
- [15] Y. Dong, R. Song, H. Liu. Bridges Structural Health Monitoring and Deterioration Detection-Synthesis of Knowledge and Technology. Final Report. Fairbanks, **2010**.
- [16] Z. Zhou, M. Huang, J. He, G. Chen, J. Ou, *Cold Reg. Sci. Technol.* **2010**, 61(1), 1.
- [17] E. Pruett, A. Phil, B. M. Holt, J. A. Sherritt, in *SPE Western Regional/AAPG Pacific Section Joint Meeting. Soc. Petrol. Eng.*, Jan **2002**.
- [18] P. Thodi, M. Paulin, D. DeGeer, M. Squires. in *OTC Arctic Technology Conference. Offshore. Technol. Conf.*, March **2015**.
- [19] S. Jeong, J. Byun, D. Kim, H. Sohn, I. H. Bae, K. H. Law, in *SPIE Smart Structures and Materials+ Nondestructive Evaluation and Health Monitoring. Int. Soc. Optic. Photon.* **2015** Apr 3, pp. 94350P.

- [20] H. S. Park, Y. Shin, S. W. Choi, Y. Kim, *Sensors* **2013**, *13*(7), 9085.
- [21] O. Lopez, A. Amy-Klein, M. Lours, C. Chardonnet, G. Santarelli, *Appl. Phys. B: Lasers Opt.* **2010**, *98*(4), 723.
- [22] O. Lopez, A. Haboucha, B. Chanteau, C. Chardonnet, A. Amy-Klein, G. Santarelli, *Opt. Express* **2012**, *20*(21), 23518.
- [23] J. L. Hulsey, F. Xiao, J. D. Dolan. Phase II: Chulitna River Bridge Structurally Health Monitoring Alaska Bridge 255–Chulitna River Bridge. Jan **2015**.
- [24] J. L. Hulsey, P. P. Brandon, F. Xiao. Sensor Selection and Field Installation Report. AUTC/AKDOT&PF Research Report. Alaska Department of T **2012**.
- [25] Y. Xia, B. Chen, S. Weng, Y. Q. Ni, Y. L. Xu, *J. Civil Struct. Health Monit.* **2012**, *2*(1), 29.
- [26] S. Alampalli, in *Proceedings-spie the International Society for Optical Engineering. Spie Int. Soc. Opt.*, **1998** Feb, Vol. 1, pp. 111.
- [27] H. Li, S. Li, J. Ou, H. Li, *Struct. Control Health Monit.* **2010**, *17*(5), 495.
- [28] H. Sohn, M. Dzwonczyk, E. G. Straser, A. S. Kiremidjian, K. H. Law, T. Meng, *Earthq. Eng. Struct. Dyn.* **1999**, *28*(8), 879.
- [29] H. Sohn, *Philos. Trans. R. Soc. A Math. Phys. Eng. Sci.* **2007**, *365*(1851), 539.
- [30] J. Hulsey, L. Yang, L. Raad, *Trans. Res. Record: J. Trans. Res. Board* **1999**, *1*(1654), 141.
- [31] M. Shulski, G. Wendler, *The Climate of Alaska*, University of Alaska Press, Fairbanks **2007**.

How to cite this article: Xiao F, Hulsey JL, Balasubramanian R. Fiber optic health monitoring and temperature behavior of bridge in cold region. *Struct Control Health Monit.* 2017;e2020. <https://doi.org/10.1002/stc.2020>